Molecular Neurobiology (2019) 56:1870–1882
https://doi.org/10.1007/s12035-018-1162-1

Wnt-7a Stimulates Dendritic Spine Morphogenesis and PSD-95 Expression Through Canonical Signaling

Eva Ramos-Fernández[1] · Cheril Tapia-Rojas[1] · Valerie T. Ramírez[1] · Nibaldo C. Inestrosa[1,2,3]

Received: 23 March 2018 / Accepted: 30 May 2018 / Published online: 2 July 2018

Abstract

Wnt signaling regulates brain development and synapse maturation; however, the precise molecular mechanism remains elusive. Here, we report that Wnt-7a stimulates dendritic spine morphogenesis in the hippocampus via glycogen synthase kinase-3 β (GSK-3β) inhibition, triggering β-catenin/T cell factor/lymphoid enhancer factor (TCF/LEF)-dependent gene transcription and promoting postsynaptic density-95 (PSD-95) protein expression. In addition, wild-type mice treated with an inhibitor of β-catenin/TCF/LEF-mediated transcription showed a reduction in spatial memory acquisition accompanied by a reduction in PSD-95 and decreases in spine density measured by Golgi staining, suggesting that PSD-95 is a novel Wnt target gene. Together, our data strongly demonstrate that Wnt-dependent target gene transcription is essential to hippocampal synaptic plasticity.

Keywords Wnt signaling · Dendritic spine plasticity · PSD-95 · TCF/LEF

Introduction

Wnt ligands are secreted glycoproteins that modulate different aspects of brain development, including synapse formation, transmission, remodeling, and adult neurogenesis [1, 2]. Additionally, the deregulation of Wnt signaling correlates with several neurological and psychiatric disorders, including schizophrenia, anxiety, and Alzheimer's disease [3, 4].

Wnt ligands act through different well-characterized signaling pathways, the canonical Wnt/β-catenin pathway and the two non-canonical pathways, Wnt/Ca^{2+} and Wnt/PCP. The Wnt/β-catenin pathway involves the binding of Wnt ligands to Frizzled receptors and low-density lipoprotein receptor-related protein 6 (LRP6) co-receptors. This binding leads to the phosphorylation of disheveled (Dvl) and the subsequent inhibition of glycogen synthase kinase-3 β (GSK-3β), inducing the accumulation of β-catenin in the cytoplasm and its translocation to the nucleus. In the nucleus, β-catenin interacts with T cell factor/lymphoid enhancer-binding factor (TCF/LEF) and activates the transcription of Wnt target genes such as Ca^{2+}/calmodulin-dependent protein kinase IV (CaMKIV) and c-Jun [5, 6]. The Wnt/Ca^{2+} signaling pathway involves intracellular Ca^{2+} mobilization and Ca^{2+}/calmodulin-dependent protein kinase II (CaMKII) and protein kinase C (PKC) activation [7], and through Frizzled and Dvl, the Wnt/PCP pathway activates Rho and Rac small GTPases [8].

It is well established that both Wnt/β-catenin and Wnt/Ca^{2+} or PCP signaling play a major role in the regulation of synaptic plasticity in the hippocampus. Classically, Wnt-5a regulates postsynaptic density through the non-canonical Wnt/Ca^{2+} pathway [9–11], while Wnt-3a and Wnt-7a, being canonical pathway effectors, modulate the pre-synaptic terminal. Specifically, Wnt-3a regulates long-term potentiation (LTP) and neurogenesis via Wnt/β-catenin signaling [12], whereas Wnt-7a plays a role in the pre-synaptic regulation of excitatory synapses in the hippocampus [13, 14] and influences memory formation [15]. In addition, GSK-3β kinase also plays an important role in synaptic formation; it has been shown that a lack of GSK-3β expression causes synaptic loss

Electronic supplementary material The online version of this article (https://doi.org/10.1007/s12035-018-1162-1) contains supplementary material, which is available to authorized users.

✉ Nibaldo C. Inestrosa
ninestrosa@bio.puc.cl

[1] Centro de Envejecimiento y Regeneración (CARE UC), Laboratorio de Neurobiología Molecular, Departamento de Biología Celular y Molecular, Facultad de Ciencias Biológicas, Pontificia Universidad Católica, 8331150 Santiago, Chile

[2] Center for Healthy Brain Ageing, School of Psychiatry, Faculty of Medicine, University of New South Wales, Sydney, NSW, Australia

[3] Centro de Excelencia en Biomedicina de Magallanes (CEBIMA), Universidad de Magallanes, 6200000 Punta Arenas, Chile

in the hippocampus [16]. In fact, we have previously shown that Andrographolide (ANDRO), a non-ATP competitive GSK-3β inhibitor [17], activates Wnt/β-catenin with positive effects on memory in vivo [18]. Additionally, inhibiting Wnt/β-catenin signaling via Dickkopf1 (Dkk-1) produces deficits in memory recognition and long-term memory [19, 20].

In the present study, we aimed to establish the role of Wnt/β-catenin signaling in the regulation of the postsynaptic region in the hippocampus. Our in vitro results reveal for the first time that canonical Wnt signaling activation by Wnt-7a and ANDRO increased dendritic protrusion density in a β-catenin-dependent manner. While Ciani et al. described a novel role for Wnt7a in increasing dendritic spine density through a calcium non-canonical pathway, here, we demonstrate that the canonical pathway played a role in Wnt7a-mediated spine formation [21]. We propose that PSD-95, one of the most abundant proteins in the postsynaptic region, is a canonical Wnt target gene based on our findings that Wnt-7a treatment increased PSD-95 protein expression and that, remarkably, genetic truncation of β-catenin in its ΔTCF/LEF binding domain reduced PSD-95 expression. In addition, inhibition of the Wnt/β-catenin cascade in vivo, using a Wnt/β-catenin/TCF-mediated transcription inhibitor (ICG), decreased spine density, altered spine morphology in the hippocampus, reduced PSD-95 protein levels, and impaired spatial memory in 3-month-old wild-type (WT) mice. Together, these findings demonstrate that Wnt/β-catenin signaling is mediated by Wnt-7a and that transcription of Wnt target genes plays a crucial role in post-synaptic dendrite formation and maturation.

Materials and Methods

Reagents and Antibodies

Recombinant Wnt-7a (rWnt-7a; 3008-WN) was purchased from R&D Systems (MN, USA). SB 216763 (SB; Cat. S3442) and ANDRO (catalog number 365645) were obtained from Sigma Chemical Company (St. Louis, MO, USA). ICG (catalog number 2275) was obtained from BioVision Inc. (CA, USA). The primary antibodies used for Western blot were as follows: mouse anti-β-actin clone AC-15 (1/10000, Sigma-Aldrich, A1978); monoclonal anti-α-tubulin antibody (1/5000, Sigma-Aldrich, T5168); anti-GSK-3β pSer-9 (1/1000, Cell Signaling Technology, #9336S); anti-GSK-3β Y216P (1/200, Santa Cruz Biotechnology, Inc., sc-11758); total GSK-3β (1/500, Abcam ab93986; 1/1000, Santa Cruz Biotechnology, Inc., sc-9166); anti-β-catenin (1/200, Santa Cruz Biotechnology, Inc., sc-7199): anti-PKCβII S660P (1/10000, Abcam ab75837); total PKCβII (1/500, Santa Cruz Biotechnology, Inc., sc-210); anti-JNK T183P/Y185P (1/1000, Cell Signaling Technology, #9251S); total JNK (1/1000, Cell Signaling Technology, #9252); anti-CaMKII T268P (1/1000, Abcam ab5683); total CaMKII (1/1000, Thermo Scientific, MA1-048); Cyclin D1 (1/200; Santa Cruz Biotechnology, Inc., sc-450); c-Jun (1/1000, Santa Cruz Biotechnology, Inc., sc-1694); CaMKIV (1/1000, Abcam, ab3557); and PSD-95 (1/1000, Abcam ab2723). PSD-95 (1/50, Santa Cruz Biotechnology, Inc., sc-32290) was used for immunofluorescence.

Hippocampal Neuronal Cultures

Rat hippocampal cultures were prepared from embryonic day 18 Sprague-Dawley rats, as described previously [22]. Briefly, hippocampi were removed and resuspended in HBSS with 0.25% trypsin and incubated for 15 min at 37 °C. After three washes with HBSS, the tissues were mechanically dissociated in Dulbecco's modified Eagle's medium (GIBCO) supplemented with 10% horse serum (GIBCO), 100 U/ml penicillin, and 100 μg/ml streptomycin. Dissociated hippocampal cells were seeded onto poly-L-lysine-coated wells. Cultures were maintained in Neurobasal growth medium (GIBCO) supplemented with B27 (GIBCO), 2 mM L-glutamine, 100 U/ml penicillin, and 100 μg/ml streptomycin. On day 2, the cultured neurons were treated with 2 μM cytosine arabinoside for 24 h. This method resulted in cultures highly enriched in neurons (~5% glia).

Plasmids

HT22 cells were transfected with empty pRK5 vector, pRK5 encoding wild-type β-catenin (β-cat WT), β-catenin with alanine mutations at all three phosphorylation sites (β-cat ΔGSK) (Ser33, Ser37 and Thr41) or β-catenin mutated at the TCF/LEF (β-cat ΔTCF) which contains a 26 amino acid neoepitope disturbing it TCF/LEF consensus site (GTTTGTT) that abolishes β-catenin transactivation ability and therefore not activate β-catenin-dependent transcription of Wnt target genes [17].

Neuronal Transfection, Treatments, and Imaging Analysis

To transfect the cultured neurons, the neurons were seeded on 35-mm poly-L-lysine-coated coverslips at a density of 60,000 cells/well. At 10 days in vitro (DIV), neurons were transfected using NeuroMag (OZ Bioscience) with EGFP plasmid (Clontech) along with the empty pRK5 vector or β-cat WT, β-cat ΔGSK or β-cat ΔTCF [23, 24]. First, the neurons were washed for 30 min with Neurobasal medium, while 0.8 μg of DNA was mixed with 1.25 μl of magneto beads and incubated for 15 min in 100 μl of Neurobasal medium. In the co-transfection experiments, the mix was prepared using 0.4 μg

of EGFP plus 0.4 μg of pRK5, β-cat WT, β-cat ΔGSK or β-cat ΔTCF, and 1.25 μl of beads. Next, the mix was added to the neurons for 15 min with the magnet in the bottom of the plate. The mix was removed 40 min later, and the transfection medium was replaced with fresh medium. At 14 DIV, the hippocampal neurons were washed in Neurobasal medium and maintained for 1 h. Next, the neurons were treated with rWnt-7a (8 or 13 nM), ANDRO (10 μM), and SB (68 nM), with or without DKK (100 ng/ml) or ICG001 (50 μM) for different time periods. An Olympus Fluo View FV 1000 confocal microscope was used to obtain digital images at a pixel resolution of 1024 pixels × 1024 pixels. To quantify the dendritic spines, the Z-stack images were reconstructed using the super-pass module of the Imaris software. The dendritic shafts and spines were manually traced using the filament mode. Protrusions less than 2 μm long (to discard filopodia) were considered for three-dimensional reconstruction. Ten neurons were imaged for each condition in three to five independent experiments. The spine density was calculated by measuring the total number of spines/dendrite length (spine density, n° spines/10 μm) for each condition.

Immunoblotting

Cells were washed with PBS and immediately processed. Briefly, cells were gently homogenized in Triton buffer supplemented with a protease inhibitor mixture and phosphatase inhibitors (25 mM NaF, 100 mM Na_3VO_4, 1 mM EDTA, and 30 μM $Na_4P_2O_7$) on a rocker shaker for 30 min at 4 °C. Protein samples were centrifuged twice at 14,000 rpm at 4 °C for 10 min. The hippocampus of the treated or control WT mice was dissected on ice and immediately processed as previously described [25]. Briefly, the hippocampal tissue was homogenized in RIPA buffer (10 mM Tris-Cl, pH 7.4, EDTA 5 mM, 1% NP-40, 1% sodium deoxycholate, and 1% SDS) supplemented with a protease inhibitor mixture and phosphatase inhibitors (25 mM NaF, 100 mM Na_3VO_4, and 30 μM $Na_4P_2O_7$) using a Potter homogenizer and then sequentially passed through syringes of different calibers. The protein samples were centrifuged twice at 14,000 rpm for 20 min at 4 °C. The protein concentrations were determined using the BCA Protein Assay Kit (Pierce). The samples were resolved by SDS-PAGE, followed by immunoblotting on PVDF membranes.

Immunofluorescence

Neurons transfected with EGFP plus pRK5 empty vector or β-cat ΔTCF were washed twice with PBS Ca^{2+}/Mg^{2+}. Then, 4% PFA-sucrose was added at room temperature (RT) for 20 min to fix the neurons. PBS washes were performed three times, and the neurons were permeabilized for 5 min in PBS-0.2% Triton. After the PBS washes, the neurons were incubated with blocking solution (PBS-2% BSA) for 30 min at 37 °C. The cells were incubated with PSD-95 primary antibody overnight at 4 °C in a wet chamber. The next day, three PBS washes were performed, and secondary antibody coupled to Alexa 555 nm (Abcam ab150110) fluorescence in a 1/500 dilution was applied for 30 min at 37 °C. Coverslips were mounted over porta objects on 5 μl of fluoromount solution. A Nikon spectral confocal microscope was used to obtain the digital images at a pixel resolution of 1024 pixels × 1024 pixels with a × 60 oil objective. Five images and at least three neurites/photo were analyzed for each condition.

RNA Extraction, Retrotranscription, and Quantitative PCR

RNA extraction was performed via the Trizol method from 500,000 neurons/well that were untreated or treated with ICG (2275 BioVision Inc.). The extracted RNA was then quantified with a NanoDrop device, and 2 μg was used for retrotranscription with SuperscriptIII (1843289 Invitrogen). Primers for the quantitative PCR for PSD-95 (Fw: 5′-ATTTTTATCACCAAGATCATTCCT -3′; Rv: 5′-CCATGACCTTTTCGGCTG -3′) were designed and obtained from IDT. The results were evaluated with the 2ΔΔCT method and normalized to GAPDH levels.

In Silico Analysis of TCF/LEF Responsive Elements

The PSD-95 promoter (2000 bp) from the three different species was analyzed with the MatInspector Module of the Genomatix Software using the following parameters: transcription binding site library, vertebrate matrix, and a 0.75 of core similarity.

Animals and Treatments

Three-month-old wild-type (WT) mice ($n = 6$ per group) were treated and handled according to the National Institutes of Health guidelines (NIH, Baltimore, MD). Intraperitoneal (IP) injections of ICG (60 mg/kg) with saline solution as the vehicle were administered three times per week. WT, control animals, were injected with vehicle only. Both experimental groups were treated for 5 weeks beginning at 3 months of age. We evaluated the general condition of the animals after the treatment following the protocol described in the *Handbook of Laboratory Animal Management and Welfare* (edited by S. Wolfensohn and M. Lloyd, Oxford University Press, 1994). The animal conditions were evaluated as follows: normal, score of 0 to 4 points; needing surveillance (consider analgesic administration), 5 to 8 points; and intense suffering that required subcutaneous analgesic injection (2 mg/kg ketoprofen every 12 h; considering euthanasia). At

scores 13 to 16, euthanasia was required (200 mg/kg ketamine and 20 mg/kg xylazine). These data are included in Table 1.

Behavioral Testing

Memory flexibility tests were performed as previously described [25]. Briefly, a circular white pool was prepared with non-toxic white paint plus a hidden platform (diameter, 9 cm) in four quadrants; the water temperature was maintained between 18 and 20 °C. Animals were pre-trained in this pool (without the platform) for 60 s 1 day before testing to acclimate the animals to the room and the swimming strategy. Then, animals were subjected to testing for four consecutive days with a maximum of 15 trials per day. Every day, the platform position in a quadrant was changed. Testing stopped when the animal reached the platform on three consecutive trials with an average of 20 s or less. The data are presented as the number of trials after which animals reached the criterion.

Golgi Staining

Golgi staining was developed using the FD Rapid GolgiStain Kit (FD NeuroTechnologies, Inc., Ellicott City, MD), an improved Golgi-Cox impregnation method to stain mature neurons. The protocol was performed according to the manufacturer's instructions [26]. Ten to twelve images were acquired

Table 1 Animal welfare. The table includes the evaluation of weight variation, physical appearance, and spontaneous behavior from all injected animals. Normal animals have scores between 0 and 4

Treatment	Control																				ICG																			
Week	1st				2nd				3rd				4th				5th				1st				2nd				3rd				4th				5th			
Mice	1	2	3	4	1	2	3	4	1	2	3	4	1	2	3	4	1	2	3	4	1	2	3	4	1	2	3	4	1	2	3	4	1	2	3	4	1	2	3	4
Weight loss																																								
0 (normal)	0	0	0	0	0	0	0	0	0	0	0	0	0	0	0	0	0	0	0	0	0	0	0	0	0	0	0	0	0	0	0	0	0	0	0	0	0	0	0	0
1 (< 10%)																																								
2 (10–20%)																																								
3 (> 20%)																																								
Physical appearance																																								
0: normal	0	0	0		0	0	0	0	0	0	0	0	0	0	0	0	0	0	0	0	0	0	0	0	0	0	0	0	0	0	0	0	0	0	0	0	0	0	0	0
1: matt hair, bad conditions																																								
2: cutaneous injures				2																																				
3: lateral decubitus, respiration by mouth																																								
Spontaneous behavior																																								
0: erect, good interaction with partners	0	0	0	0	0	0	0	0	0	0	0	0	0	0	0	0	0	0	0	0		0	0	0	0	0	0	0	0	0	0	0	0	0	0	0	0	0	0	0
1: lethargy, less active, mobility difficulty																					1																1			
2: low mobility and low alarm state																																								
3: automutilation, weird vocalization, immobility, anxious																		3																						
Behavior vs. stimuli																																								
0: alert, responsive, mobility without difficulty	0	0	0	0	0	0	0	0	0	0	0	0	0	0	0	0	0	0	0	0	0	0	0	0	0	0	0	0	0	0	0	0	0	0	0	0	0	0	0	0
1: behavioral alterations, coordination loss and ataxia																																								
2: unusual behavior and movements																																								
3: convulsions, comatose animal																																								

from three different slices from four animals in each group using the × 100 objective of an Olympus Stereologic microscope (from the UC Advanced Microscope unit). To analyze the number and type of spines, we used Reconstruct software. Two dendrites from each image were analyzed from each animal.

Statistical Analyses

The results are presented as a graph depicting the mean ± SEM. Statistical significance was determined using a one-way ANOVA with a Bonferroni post hoc test for multiple comparisons or Student's *t* test for two-group comparisons. *P* values ≤ 0.05 were regarded as significant. In the figures, *P* values between 0.01 and 0.05 are indicated with one asterisk, *P* values between 0.001 and 0.01 are indicated with two asterisks and *P* values less than 0.001 are indicated with three asterisks. All statistical analyses were performed using Prism software (GraphPad Software, Inc.)

Results

Wnt-7a Activates the Canonical Wnt Signaling Pathway and Regulates Dendritic Protrusion Density

We evaluated whether the canonical Wnt pathway is activated after the Wnt-7a stimulation of hippocampal neurons. We measured key components, such as β-catenin levels, GSK-3β inhibition, and the Wnt target gene CaMKIV. When hippocampal cultured neurons were exposed to Wnt-7a (for 3 or 16 h at 13 nM), β-catenin, CaMKIV, and GSK-3β Ser-9 phosphorylation (inactive form) levels were increased compared with those in the control (Fig. 1a), indicating that Wnt-7a activates the canonical Wnt pathway in hippocampal neurons, as reported previously [13].

To examine the effect of Wnt-7a on dendritic spine morphogenesis in cultured hippocampal neurons, we transfected neurons at 10 DIV with enhanced green fluorescent protein plasmid (EGFP) to evaluate neuronal morphology. Dendritic protrusions were analyzed using Imaris software to determine dendritic spine density. We considered the protrusion mature spines because they were PSD-95-positive (Fig. 1b). Hippocampal neurons exposed to 13 nM rWnt-7a exhibited increased dendritic spine density after 3 and 16 h of treatment (Fig. 1c). Next, we aimed to determine whether the blockade of Wnt canonical signaling affects the Wnt-7a-dependent increase in dendritic spines. The Dkk family of proteins act as antagonists of canonical Wnt signaling by binding to LRP5/6 to prevent the interaction between Wnt and Frizzled receptors [27]. Interestingly, the exogenous addition of Dkk-1 for 3 h inhibited the Wnt-7a-mediated increase of β-catenin (Fig. 2a). GSK-3β-ser-9 phosphorylation was also prevented by Dkk-1 treatment (Fig. 2a), indicating that the Wnt-7a activation of Wnt canonical signaling requires ligand-receptor binding.

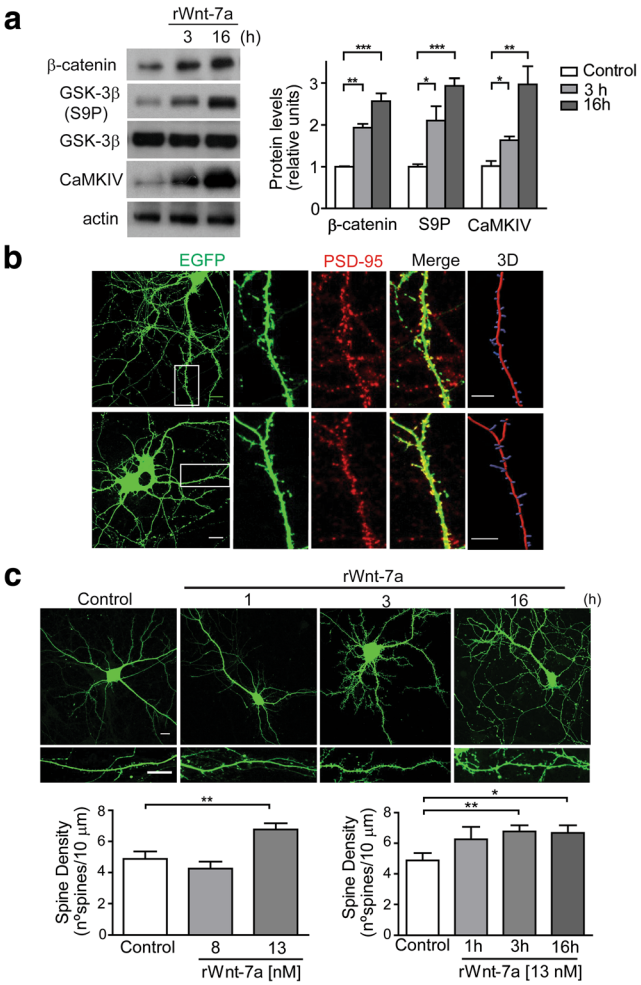

Fig. 1 Wnt-7a activates Wnt canonical signaling and modulates dendritic spine morphogenesis in cultured hippocampal neurons. **a** Representative immunoblots and quantification of protein extracted from hippocampal neuronal cultures at 14 DIV treated with recombinant Wnt-7a (rWnt-7a; 13 nM) for 3 or 16 h or with control for 16 h ($n = 4$). **b** Immunodetection of PSD-95 (red) in EFGP-transfected neurons (green) at 14 DIV. The merged image shows the EGFP protrusions with the PSD-95 puncta staining in the head, indicating that the protrusions are spines. 3D: three-dimensional reconstruction of the dendrite. **c** Representative images and quantification of the protrusion density vs. concentration (after 3 h of treatment) or time of rWnt-7a treatment (at 13 nM) in EGFP-transfected neurons. Scale bar, 10 µm; inset, 10 µm ($n = 4$; 10 neurons/condition, 3 neurites/neuron). $^{**}p < 0.01$; $^{*}p < 0.05$

Moreover, treatment with Dkk-1 blocked the Wnt-7a-mediated increase in dendritic spine density, while Dkk-1 significantly reduced the number of dendritic spines when used alone (Fig. 2b). Taken together, our results suggest that activation of Wnt canonical signaling mediates dendritic spine formation induced by the Wnt-7a in hippocampal neurons.

GSK-3β Inhibition Mimics the Wnt-7a Modulation of Dendritic Protrusion

To dissect the role of Wnt canonical signaling on dendritic spine regulation in hippocampal cultured neurons, we

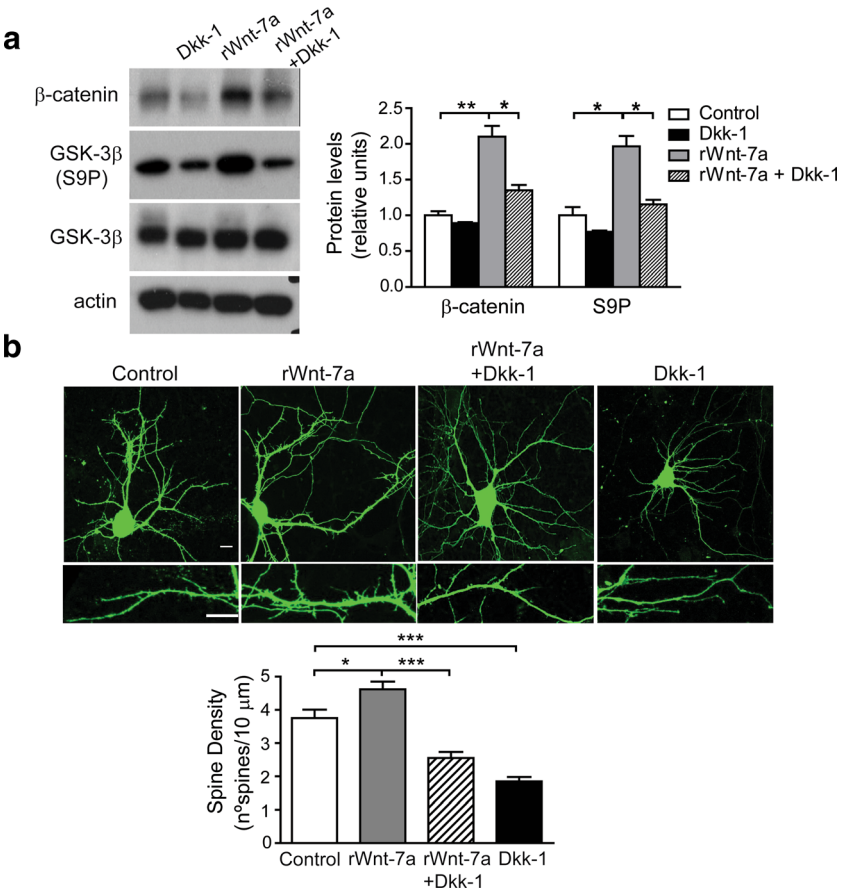

Fig. 2 Dkk-1 impedes Wnt canonical pathway activation and dendritic spine formation. **a** Immunoblots and quantification of protein extracted from hippocampal cultured neurons treated with rWnt-7a and/or Dkk-1 (100 ng/ml) for 3 h. **b** Representative images and quantification of EGFP-transfected hippocampal neurons treated at 14 DIV for 3 h with rWnt-7a (13 nM) and/or Dkk-1 (100 ng/ml). Quantification shows the spine density as the number of spines per 10 μm of neurite length. Scale bar, 10 μm; inset, 10 μm ($n = 3$–5 neurons/condition, 3 neurites/neuron). ***$p < 0.001$; **$p < 0.01$; *$p < 0.05$

evaluated the effect of ANDRO, a GSK-3β substrate-competitive inhibitor [17]. We found that ANDRO induced GSK-ser9 phosphorylation, increased β-catenin level and finally increased CaMKIV expression in hippocampal neurons (Fig. 3a). Additionally, ANDRO recapitulated the Wnt-7a-dependent increase in spine density growth after 3 and 16 h of treatment (Fig. 3b). This effect was also observed after treatment with SB216763 (SB) (Fig. 3c), another ATP-competitive GSK inhibitor [28]. These results suggest that Wnt-7a acts through the GSK-3β pathway, promoting spine density enlargement and altering the expression of Wnt target genes in hippocampal neurons.

Wnt-7a/GSK-3β Signaling Requires β-catenin/TCF-Mediated Transcription to Regulate Dendritic Spine Density in Cultured Hippocampal Neurons

The canonical Wnt pathway ultimately produces changes in several target genes that lead to functional and structural changes in a cell context-dependent manner [29]. Gene expression changes are dependent on the translocation of β-catenin to the nucleus where it binds to TCF/LEF regions. To determine whether β-catenin/TCF/LEF gene transcription is required for Wnt-7a-spine regulation, we used ICG-001 (ICG), an antagonist of β-catenin TCF-mediated transcription [30]. As expected, ICG treatment decreased CaMKIV levels (Fig. 4a). Interestingly, spine density was also affected, decreasing after 16 h of ICG treatment (Fig. 4b). These results suggest that inhibition of canonical Wnt signaling at the gene transcription level reduces the basal number of dendritic protrusions. To determine the contribution of β-catenin/TCF activation to the effect of Wnt-7a/GSK-3β activation on spine density, neurons were co-treated with ICG and Wnt-7a or ANDRO for 16 h. ICG co-treatment prevented the effects of Wnt-7a and ANDRO on CaMKIV expression (Fig. 4c) and, importantly, on dendritogenesis (Fig. 4d). Thus, β-catenin-dependent-gene transcription is required for Wnt-7a/GSK-3β-mediated dendritic protrusion increases in vitro.

Wnt Canonical Pathway Regulates PSD-95 Expression in Cultured Hippocampal Neurons

Given the strong blocking effect of ICG on dendritic spine density, we examined the potential effect of Wnt-7a signaling on PSD-95 expression. We observed that the Wnt-7a ligand increased the expression of PSD-95 protein after 3 and 16 h of treatment (Fig. 5a). Moreover, Dkk-1 and ICG treatment for 24 h decreased PSD-95 expression in a concentration-dependent manner (Fig. 5c). Expression of the canonical

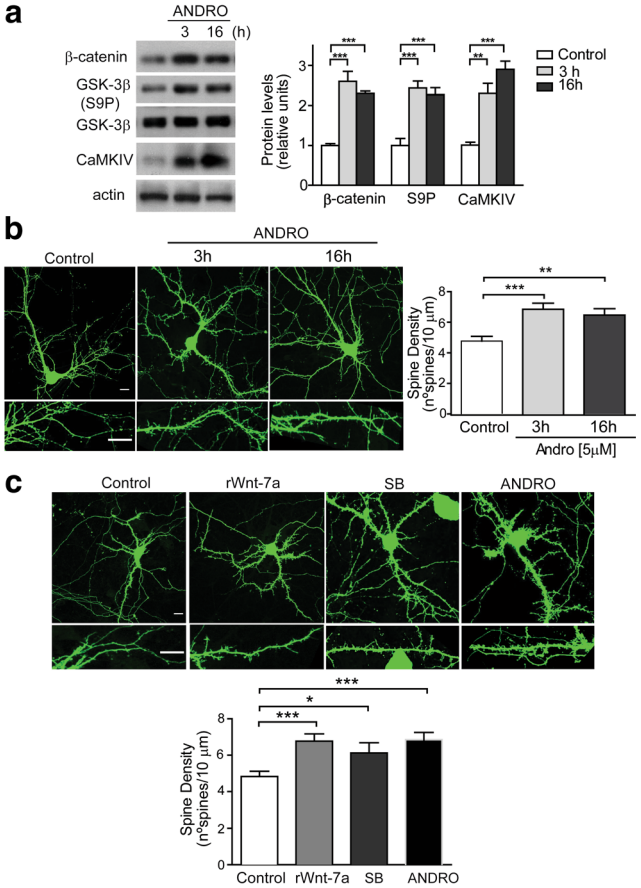

Fig. 3 GSK-3β inhibition is sufficient to activate the Wnt canonical signaling pathway and to increase dendritic spine density. **a** Representative Western blots and quantification of total GSK-3β, phosphorylated levels of GSK-3β (S9P; $n = 3$), and total levels of β-catenin ($n = 3$) and CaMKIV ($n = 3$) in neurons incubated with ANDRO (10 μM) for 3 or 16 h. Actin was used as the loading control. **b** Representative images of DIV14 hippocampal neurons (transfected with EGFP on DIV10) and treated with ANDRO 5 μM for 3 or 16 h. Quantification shows spine density (no. of spines per 10 μm of neurite length). Scale bar, 10 μm; inset, 10 μm ($n = 4$ independent experiments). $^{***}p < 0.001$; $^{**}p < 0.01$. **c** EGFP-transfected hippocampal neurons treated with rWnt-7a, or one of two GSK-3β inhibitors (SB or ANDRO). Quantification shows the spine density after each treatment. Scale bar, 10 μm; inset, 10 μm. ($n = 4$; 10 neurons/condition, 3 neurites/neuron). $^{***}p < 0.001$; $^{*}p < 0.05$

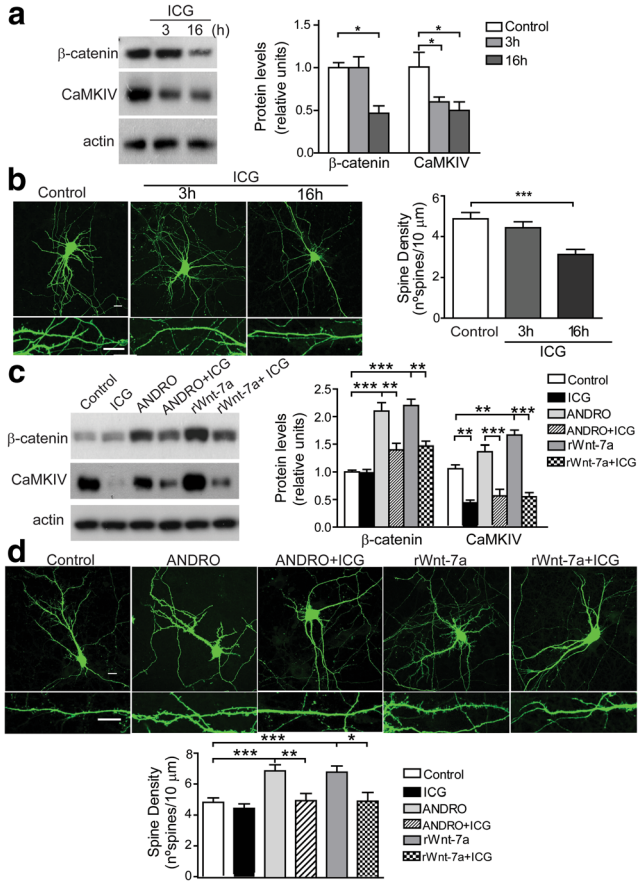

Fig. 4 ICG treatment blocks Wnt-7a signaling pathway and the increase in dendritic spine density in hippocampal neurons. **a** Representative immunoblot and quantification of total β-catenin and CaMKIV protein levels in cultured hippocampal neurons at DIV 14 treated with ICG (50 μM) for 3 or 16 h. Actin was used as the loading control ($n = 3$). **b** Representative images and quantification of the density of dendritic protrusions versus time of treatment with ICG and control from EGFP-transfected neurons ($n = 4$). **c** Representative immunoblots and quantification of total β-catenin and CaMKIV levels from neurons treated with control, ICG, ANDRO or rWnt-7a or co-treated with ANDRO/ICG-001 or rWnt7a/ICG-001 for 3 h ($n = 3$). Images and quantification of dendritic protrusions from EGFP-transfected neurons treated with the same conditions as **c**. Scale bar, 10 μm; inset, 10 μm ($n = 5$; 10 neurons/condition, 3 neurites/neuron). $^{***}p < 0.001$; $^{**}p < 0.01$; $^{*}p < 0.05$

Wnt target gene c-Jun was also reduced following both treatments (Fig. 5c and Supplementary Fig. 1), while β-catenin accumulation decreased only under ICG treatment (Fig. 5c). In addition, rat hippocampal neurons treated with 50 μM ICG for 24 h shown a significant reduction of PSD-95 mRNA levels (Fig. 5b). These data suggest that neuronal expression of PSD-95 could be under the control of canonical Wnt signaling. In silico analysis of the PSD-95 promoter sequence (considering only the 2000 bp upstream from the first ATG) of human, rat, and mouse showed TCF/LEF motifs respectively as follows: four [located in the 209 to 225 (negative strand), 225 to 241 (positive strand), 1765 to 1781 (negative strand) and 1974 to 1990 positions (negative strand)], one [located in the 341 to 357 position (negative strand)], and two [located in the 154 to 170 (positive strand) and 335 to 351 positions (negative strand)]. Figure 5d shows the 2000 bp previous to the PSD-95 codifying sequence from the three species and the respective locations of the putative TCF/LEF motifs. Finally, to demonstrate that PSD-95 expression and spine formation are β-catenin/TCF/LEF-dependent, we transfected neurons either with a plasmid overexpressing a mutant of β-catenin that abolishes its transactivation ability (β-cat ΔTCF), β-catenin WT, or β-cat ΔGSK that possesses a mutation in the GSK-3β-binding region [23]. Our results show that β-cat ΔTCF reduced the PSD-95 protein expression in the HT22 cell line (Fig. 5e). Overexpression of β-catenin WT also

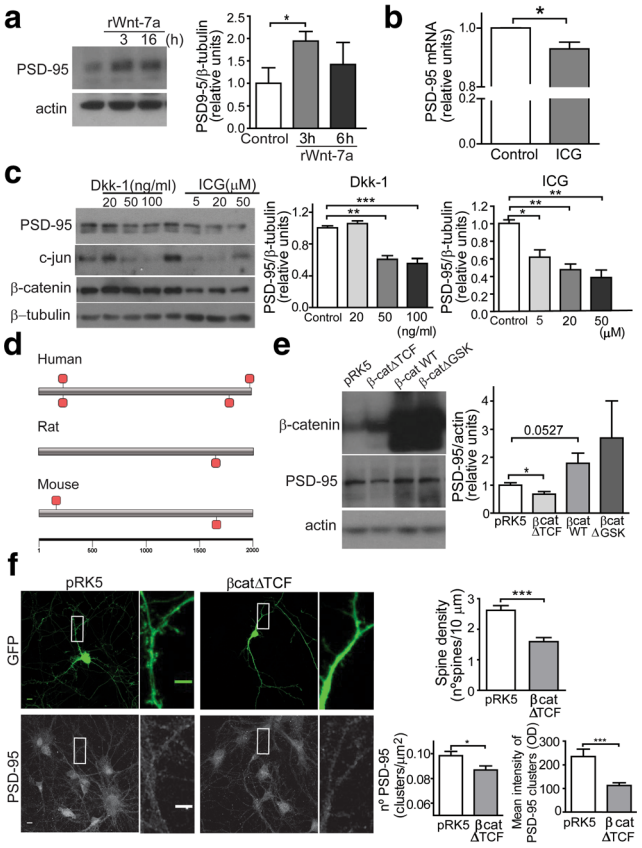

Fig. 5 Wnt canonical signaling regulates PSD-95 expression. **a** Representative blot and quantification of PSD-95 and actin levels. Protein was extracted from hippocampal cultures at 14 DIV left untreated (control) or treated with rWnt-7a (13 nM) for 3 or 16 h ($n = 3$). **b** qRT-PCR from total RNA isolated from untreated (control) hippocampal neurons or after 24 h of 50 μM ICG-treatment. PSD-95 mRNA levels were normalized to GAPDH mRNA and are expressed relative to the control condition. Bars show the mean ± SEM ($n = 3$). **c** Representative immunoblot from hippocampal neurons treated with Dkk-1 (20, 50, and 100 ng/mL) and ICG1 (5, 20, and 50 μM) for 24 h. Quantification of PSD-95 levels relative to β-tubulin amount is shown ($n = 3$). **d** Diagram showing the PSD-95 promoter sequences (2000 bp upstream from its ATG) in human, rat, and mouse. The red squares show the location of the putative TCF/LEF domains in the PSD-95 promoter sequences. **e** Representative Western blot of HT22 neurons transfected with pRK5 empty vector, β-cat ΔTCF, β-cat WT, or β-cat ΔGSK. Quantification of PSD-95 levels relative to actin levels ($n = 4$). **f** Hippocampal neurons co-transfected with GFP and pRK5 or β-cat ΔTCF. Lower panels are the immunofluorescence images showing PSD-95 in the same transfected hippocampal neurons. Quantification demonstrates the spine density (no. of spines/10 μm), the number of PSD-95 clusters/μm^2 and the mean intensity of PSD-95 clusters. Scale bar, 10 μm; inset, 5 μm. ($n = 3$; 3 neurites/1–2 neurons/5 images/condition). ***$p < 0.001$; *$p < 0.05$

displayed a tendency to increase PSD-95 expression (Fig. 5e). Interestingly, the number and the mean intensity of PSD-95 clusters were significantly reduced in β-cat ΔTCF-transfected neurons (Fig. 5f). Additionally, compared with control plasmid-transfected neurons (pRK5), β-cat ΔTCF-transfected neurons showed a significant reduction in dendritic spine density (Fig. 5f). All together, these findings strongly suggest that PSD-95 expression is regulated by the canonical Wnt signaling pathway.

ICG Inhibits the Wnt Canonical Pathway In Vivo and Alters Dendritic Spine Density and Morphology in the Hippocampus

Previous studies have shown that ICG inhibits the Wnt signaling pathway in several tissues in vivo [31]. To determine whether ICG treatment inhibits the canonical Wnt pathway in the hippocampus in vivo, we treated WT mice with ICG (60 mg/kg i.p.) for 5 weeks. No changes in weight or general animal welfare were observed (Table 1, Fig. 8c). ICG treatment reduced GSK-3β-S9 phosphorylation, β-catenin accumulation, and Cyclin D1 expression (Fig. 6a), whereas GSK-3β-Y216 phosphorylation (active form) and GSK-3β total levels were not altered (Fig. 6a). These data confirm that ICG blocks the canonical Wnt pathway in vivo in the hippocampus. Furthermore, we evaluated the non-canonical Wnt signaling pathway by measuring the phosphorylated and total levels of PKCβII-S660, CaMKII-Y286, and JNK-T183/Y185 proteins. ICG did not modify PKCβII and JNK activation; however, CaMKII activation was partially reduced (Fig. 6a).

We next examined possible defects in spine morphogenesis in ICG-treated mice. ICG-treated mice exhibited a significant decrease in the number of spines in the Cornus Ammonis 1 (CA1) region of the hippocampus (Fig. 7a, b). We classified the different types of spines following the protocol previously described [32]. We found that ICG treatment increases the percentage of thin spines (immature state of the protrusions), accompanied by a reduction in the percentage of branched spines (mature form) (Fig. 7b). Collectively, these results demonstrate that activation of the canonical Wnt signaling pathway and the transcription of Wnt target genes are required in vivo for the proper formation and growth of dendritic spines in the CA1 region.

Wnt Canonical Signaling Inhibition Reduces Spatial Memory in Mice

Changes in spine density or maturity are associated with alterations in hippocampal functions, including spatial learning and memory [33]. Therefore, we assessed hippocampal-dependent episodic memory using the memory flexibility paradigm. In this test, the animals are trained to learn a different location of the hidden platform each day [25, 34]. The analysis of behavioral performance indicates that ICG-treated mice required more trials to meet the learning criterion than control mice (Fig. 8a). No significant difference was observed in the swim velocity between the ICG- and saline-treated mice, which confirmed non-locomotor deficiency (Fig. 8b). The swim tracks depict the paths taken by the animals to reach

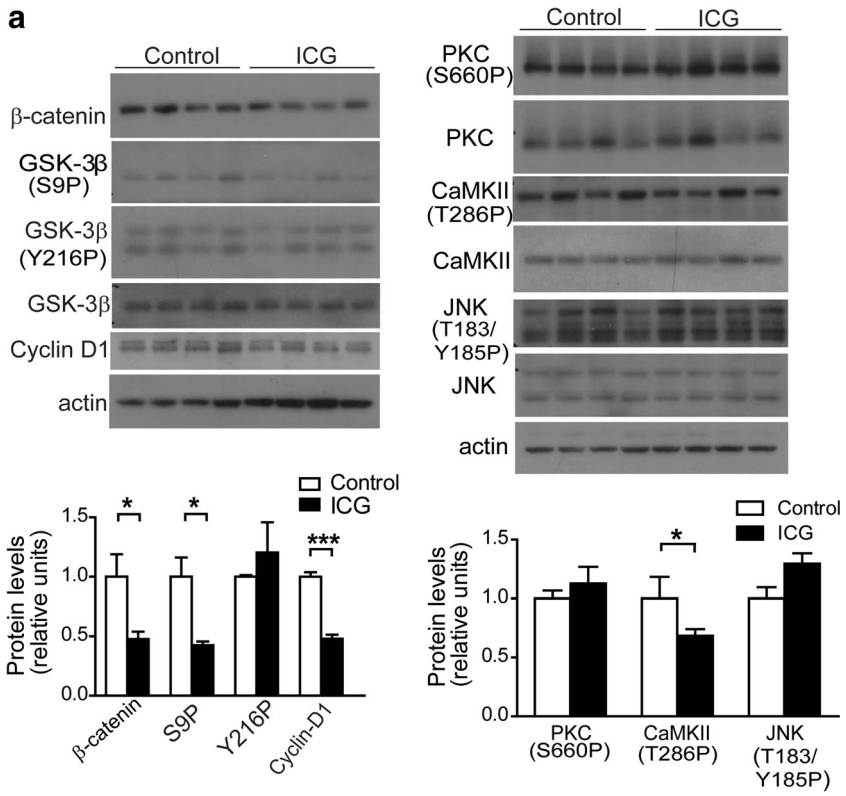

Fig. 6 Inhibition of Wnt canonical signaling in ICG-injected mice. **a** Immunoblots from the hippocampus of mice injected with saline solution (control) or with ICG. Proteins involved in the canonical pathway (β-catenin, GSK-3β S9P, GSK-3βY216P, total GSK-3β, Cyclin D1) are shown in the left panel; proteins involved in the non-canonical pathway (PKC S660P, total PKC, CaMKII T286P, total CaMKII, JNK T183/Y185P, total JNK) are shown in the right panel. Quantification shows the levels of protein relative to its loading control protein (actin, total GSK-3β, total PKC, total CaMKII, or total JNK) ($n = 4$). ***$p < 0.001$; *$p < 0.05$

the platform on the fourth trial of each day of training (Fig. 8d).

Consistent with the idea that ICG treatment causes cognitive impairment due to a reduction in the number of dendritic spines, we evaluated PSD-95 expression in the hippocampus. Interestingly, PSD-95 expression was reduced in ICG mice after 5 weeks (Fig. 8e) or 10 weeks of injection (Fig. 8f), supporting the hypothesis that Wnt canonical signaling might regulate PSD-95 expression.

Discussion

In the present study, we demonstrated that Wnt-7a, a Wnt ligand highly expressed in the hippocampus of the adult mouse [35], stimulates dendritic spine morphogenesis in hippocampal neurons through the canonical Wnt signaling pathway. We reported that Wnt-7a-induced dendritogenesis required the transcription of Wnt target genes mediated by β-catenin binding to TCF/LEF transcription factors. Among these genes, we showed for the first time that the Wnt canonical signaling pathway regulated PSD-95 expression in vitro and in vivo. Finally, we showed that the pharmacological inhibition of β-catenin binding to TCF/LEF in WT mice reduced dendritic spine density in the CA1 of the hippocampus and induced a deficit in spatial memory. Together, these data indicate that the canonical Wnt signaling pathway and Wnt-dependent target genes are necessary to promote the development of dendritic spines and memory formation in the hippocampus, stimulating PSD-95 protein expression.

In this study, we evaluated whether Wnt-7a could activate the canonical Wnt pathway. Effectively, we observed that Wnt-7a stimulated GSK-3β inhibition as indicated by the increased levels of the inactive form of GSK-3β. A similar effect was observed when we used ANDRO, a GSK-3β inhibitor previously described by our laboratory. GSK-3β inhibition stabilizes and promotes the translocation of β-catenin to the nucleus [36], and these events are necessary for the final function of the canonical pathway [37, 38]. We also observed that both the Wnt-7a ligand and ANDRO induced an increase in CaMKIV expression in primary hippocampal neurons.

Previous reports have also shown that Wnt-7a acts as a canonical Wnt ligand, and through this signaling pathway, it regulates pre-synaptic structure and function [39]. Wnt-7a increases synapsin I clustering [40, 41], increases the number of pre-synaptic sites, regulates the recycling and endocytosis of synaptic vesicles, induces neurotransmitter release [13], and improves α7-nicotinic acetylcholine receptor clustering [42]. Other reports have suggested that Wnt-7a has a post-synaptic function [21] through the activation of the calcium-non-canonical pathway and possibly participates in the process of memory formation [15]. We showed here that the Wnt-7a ligand promoted the development and maturity of dendritic spines in hippocampal neurons, as previously reported [21]; however, we further demonstrated that this process was mediated by activation of the canonical Wnt pathway. This study is

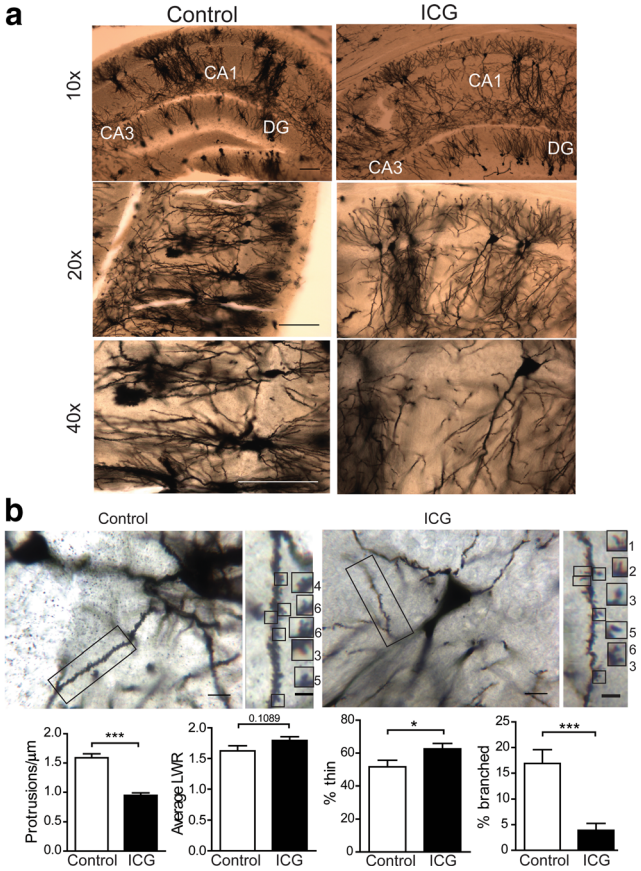

Fig. 7 ICG impairs dendritic spine formation and morphology in vivo. **a** Representative Golgi images showing the hippocampal structure from control and ICG-injected mice. In × 10 images, Cornus Ammonis 1 (CA1), CA3, and dentate gyrus (DG) regions are shown. Inset images show hippocampal neurons from the CA1 region, which were analyzed to classify and count protrusions. Scale bars, 100 µm in all images. **b** Golgi-stained neurons from mice control or injected with ICG. The graphs reflect the number of protrusions/µm, the average length/width ratio (LWR), % of thin protrusions, and % of branched protrusions. 1, filopodia (length > 2 µm); 2, long thin (length < 2 µm); 3, thin (length < 1 µm); 4, stubby (LWR < 1); 5, mushroom (> 0.6 µm); and 6, branched (2 or more heads). Scale bar, 10 µm; inset, 5 µm. ($n = 3$; 2 dendrites/1–2 neuron/4 photos/3 animal/group). ***$p < 0.001$; *$p < 0.05$

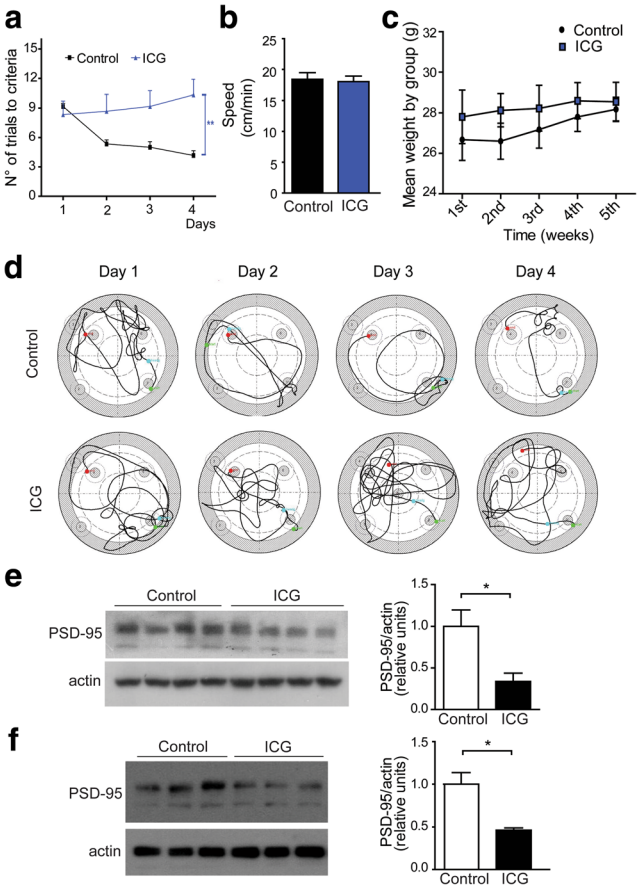

Fig. 8 Inhibition of Wnt canonical signaling impairs spatial memory in WT mice. **a** Graph showing the number of trials to criterion vs. the number of testing days in the Memory flexibility test (MF; a variant of the Morris water maze; $n = 6$). **b** Bar diagram showing the swimming speed (cm/min) of control and ICG-injected mice ($n = 6$). **c** Diagram shows the mean weight progression by group through the 5 weeks of injection. **d** Representative traces from each testing day in the MF from each treatment group. Green circles, starting point. Red circles, ending point. Light blue circles, position of the mouse head. **e** PSD-95 and actin Western blot from the hippocampus of control or ICG-injected mice after 5 weeks of treatment. Quantification shows PSD-95 relative to actin levels ($n = 4$). **f** PSD-95 and actin Western blot from the hippocampus of control or ICG-injected mice after 10 weeks of treatment. Quantification reflects PSD-95 relative to actin levels ($n = 3$). **$p < 0.01$; *$p < 0.05$

the first to demonstrate that Wnt-7a promotes dendritogenesis by activating the canonical Wnt pathway. This effect was replicated using GSK-3β inhibitors, including ANDRO and SB, and prevented by Dkk-1, an endogenous Wnt antagonist. Thus, we propose a new function of Wnt-7a in regulating postsynaptic structure.

In the literature, diverse studies discuss the role of GSK-3β in neural processes that are independent of Wnt target genes [43]. To demonstrate that the effects of canonical Wnt signaling on dendritic spine formation require the transactivation of Wnt target genes, we used ICG [30]. We observed that inhibiting β-catenin/TCF binding impedes the dendritogenic effect of Wnt-7a and ANDRO in vitro. More importantly, only ICG reduced the spine density of hippocampal neurons, strongly suggesting that ICG inhibits endogenous canonical Wnt signaling activity. Therefore, the transcription of Wnt target genes is an important regulator of the formation and maturation of dendritic spines. Our study confirms previous observations on the role of canonical Wnt signaling in the post-synaptic region and in dendritic spines.

Multiple Wnt target genes have been described [44], and many of these play key roles in the synapse [6]. For the first time, we proposed that PSD-95, the main postsynaptic scaffolding protein, could be a new β-catenin/TCF/LEF transcription target gene. We showed that PSD-95 has binding sites to TCF/LEF in its promoter and that Wnt-7a induced PSD-95 expression. In contrast, ICG and Dkk-1 reduced PSD-95 protein expression. These results were validated by a molecular

approach, using a β-catenin plasmid that was incapable of inducing the transcription of Wnt target genes (β-cat ΔTCF). This plasmid reduced the number of PSD-95 clusters and simultaneously decreased spine density in primary hippocampal cultures. Previous reports demonstrated that the complete knockout of PSD-95 in mice results in severe deficits in spatial learning and memory, demonstrating that PSD-95 is necessary for synaptic formation [45, 46]. The current results therefore indicate a new role for canonical Wnt signaling in the post-synaptic region, regulating the expression of PSD-95, which is one of the most important proteins in the synapse. Finally, to demonstrate the role of Wnt target genes in the formation and maturity of dendritic spines in vivo, we treated WT mice with ICG for 5 weeks and found severe alterations in the structure of dendritic spines. In the hippocampus of ICG-treated mice, we observed canonical Wnt signaling dysfunction, reduced spine density, and decreased PSD-95 expression, triggering impaired synaptic function and decreased spatial memory compared with that in control mice. These results suggest that Wnt target genes play an important role in the formation of dendritic spines in vivo. In fact, the role of canonical Wnt signaling in synaptic function has previously been established [44, 47, 48]. Tetanic stimulation induces Wnt-3a release [12], and Wnt signaling activation facilitates LTP processes [12, 49, 50] and LTD inhibition [50], the two main processes involved in memory formation. In contrast, inhibition of Wnt signaling impairs LTP [12]. Therefore, an important and complementary analysis could include the neuronal electrophysiological activity of the CA1 region of the hippocampus of ICG-injected mice. Future studies in our laboratory will address these experiments.

Modifications in the density, maturity, size, and shape of dendritic spines induced by activity have been linked to learning and memory processes [51]. A direct association between dendritic spine density in the CA1 region of the hippocampus and the formation of new memories has been established [52–55]. In fact, spatial working memory requires the maturity of dendritic spines to mushroom spines [51]. In contrast, decreased spine density or reduced maturity has been linked to mental retardation, memory loss, and Alzheimer's disease [56]. Our findings support the importance of dendritic spine density and maturity in memory formation and reveal the canonical Wnt signaling pathway as a new mechanism that regulates the dendritogenic process in the hippocampus.

Wnt signaling stimulates the transcription of Wnt target genes that are required for long-term memory [6]. In this study, inhibition of β-catenin-dependent Wnt signaling transcription reduced the expression of the Wnt target gene Cyclin D1 in the hippocampus and triggered severe memory deficits in WT mice. This finding confirms the importance of complete Wnt signaling activity, including the transcription of Wnt target genes, in spatial memory. Our results reinforce previous data that suggest the participation of Wnt signaling in learning and memory [15] and that the canonical Wnt pathway is required for object recognition memory [20]. PSD-95 is necessary for the appropriate formation of dendritic spines and, ultimately, memory consolidation [57, 58]. Likewise, PDZ ligand binding-deficient PSD-95 knock-in mice showed impaired synaptic clustering of PSD proteins, altered signal transmission in hippocampal neurons, and disrupted learning and memory abilities [59]. Therefore, our study demonstrates that the inability of Wnt signaling to transcribe Wnt target genes, such as CaMKIV, PSD-95 or other genes involved in the memory formation process, leads to severe hippocampus-associated cognitive alterations.

Importantly, our findings, in association with previous results reported by our laboratory and others, indicate that the Wnt-7a ligand can activate both the canonical [13, 40–42] and non-canonical Wnt pathways [21]. We found here that Wnt canonical signaling regulates PSD-95 expression. Interestingly, previous studies have indicated that the postsynaptic region, including dendritic spine morphogenesis, is related to the non-canonical pathway [1, 9]. For example, our preceding data demonstrated that Wnt-5a plays a major role by activating the non-canonical Wnt pathway, regulating the clustering of PSD-95 in hippocampal neurons [11] and spine density but not PSD-95 expression [10, 60]. Therefore, both Wnt signaling pathways could act together to regulate the structure and function of the excitatory synapses and ultimately to promote the correct architecture and function of the hippocampus modulating PSD-95 clustering and expression. The time course and duration of Wnt signaling activation in these processes, as well as the pathway crosstalk, is a matter that could be evaluated in future studies.

In conclusion, our results indicate that canonical Wnt signaling plays a key role in the formation and maturation of dendritic spines and that the transcription of Wnt target genes is necessary to promote spine density and memory in the hippocampus. In addition, our results indicate that PSD-95 is a Wnt target gene and propose a new function of the Wnt/β-catenin signaling pathway in the post-synaptic region.

Acknowledgments The authors would like to thank Dr. Caitlin S. M. Cowan (University College Cork, Ireland) for her contribution to the final version of the manuscript and Gloria Méndez for preparing the primary rat culture of hippocampal neurons. This work was supported by grants AFB 170005 and CONICYT-PFB no. 12/2007 from the Basal Center for Excellence in Science and Technology and by Fondecyt no. 1120156 to NCI, as well as by a predoctoral fellowship from the Comisión Nacional de Investigación Científica y Tecnológica (CONICYT) to V.T.R and C.T-R and postdoctoral fellowship Fondecyt Postdoctorado no. 3140355 to E.R-F.

Author Contributions NIC, CTR, VTR, and ERF designed the experiments and participated in the preparation of the manuscript. VTR performed the GFP transfections and confocal images, analyzed and interpreted results, and wrote the manuscript. CTR performed most of the Western blots, mouse injections, behavioral test analysis, and interpretation of results and wrote the manuscript. ER-F performed GFP transfections, immunofluorescence experiments, Western blots, mouse

injections, and Golgi staining, analyzed and interpreted results, composed the figures, and organized the final manuscript. NIC supervised the experiments and participated in the discussion of the results.

Compliance with Ethical Standards

The Bioethical and Biosafety Committee of the Faculty of Biological Sciences of the Pontificia Universidad Católica de Chile approved the experimental culture procedures, animal treatments and behavioral experiments.

Conflicts of Interest The authors declare that they have no competing interests.

References

1. Inestrosa NC, Arenas E (2010) Emerging roles of Wnts in the adult nervous system. Nat Rev Neurosci 11(2):77–86. https://doi.org/10.1038/nrn2755
2. Budnik V, Salinas PC (2011) Wnt signaling during synaptic development and plasticity. Curr Opin Neurobiol 21(1):151–159. https://doi.org/10.1016/j.conb.2010.12.002
3. Inestrosa NC, Montecinos-Oliva C, Fuenzalida M (2012) Wnt signaling: role in Alzheimer disease and schizophrenia. J NeuroImmune Pharmacol 7(4):788–807. https://doi.org/10.1007/s11481-012-9417-5
4. Wang J, Zhu G, Huang L, Nie T, Tao K, Li Y, Gao G (2017) Morphine administration induces change in anxiety-related behavior via Wnt/beta-catenin signaling. Neurosci Lett 639:199–206. https://doi.org/10.1016/j.neulet.2017.01.005
5. Logan CY, Nusse R (2004) The Wnt signaling pathway in development and disease. Annu Rev Cell Dev Biol 20:781–810. https://doi.org/10.1146/annurev.cellbio.20.010403.113126
6. Arrazola MS, Varela-Nallar L, Colombres M, Toledo EM, Cruzat F, Pavez L, Assar R, Aravena A et al (2009) Calcium/calmodulin-dependent protein kinase type IV is a target gene of the Wnt/beta-catenin signaling pathway. J Cell Physiol 221(3):658–667. https://doi.org/10.1002/jcp.21902
7. Kuhl M, Sheldahl LC, Park M, Miller JR, Moon RT (2000) The Wnt/Ca2+ pathway: a new vertebrate Wnt signaling pathway takes shape. Trends Genet 16(7):279–283
8. Nagaoka T, Ohashi R, Inutsuka A, Sakai S, Fujisawa N, Yokoyama M, Huang YH, Igarashi M et al (2014) The Wnt/planar cell polarity pathway component Vangl2 induces synapse formation through direct control of N-cadherin. Cell Rep 6(5):916–927. https://doi.org/10.1016/j.celrep.2014.01.044
9. Varela-Nallar L, Alfaro IE, Serrano FG, Parodi J, Inestrosa NC (2010) Wingless-type family member 5A (Wnt-5a) stimulates synaptic differentiation and function of glutamatergic synapses. Proc Natl Acad Sci U S A 107(49):21164–21169. https://doi.org/10.1073/pnas.1010011107
10. Ramirez VT, Ramos-Fernandez E, Henriquez JP, Lorenzo A, Inestrosa NC (2016) Wnt-5a/Frizzled9 receptor signaling through the G alpha(o)-G beta gamma complex regulates dendritic spine formation. J Biol Chem 291(36):19092–19107. https://doi.org/10.1074/jbc.M116.722132
11. Farias GG, Alfaro IE, Cerpa W, Grabowski CP, Godoy JA, Bonansco C, Inestrosa NC (2009) Wnt-5a/JNK signaling promotes the clustering of PSD-95 in hippocampal neurons. J Biol Chem 284(23):15857–15866. https://doi.org/10.1074/jbc.M808986200
12. Chen J, Park CS, Tang SJ (2006) Activity-dependent synaptic Wnt release regulates hippocampal long term potentiation. J Biol Chem 281(17):11910–11916. https://doi.org/10.1074/jbc.M511920200
13. Cerpa W, Godoy JA, Alfaro I, Farias GG, Metcalfe MJ, Fuentealba R, Bonansco C, Inestrosa NC (2008) Wnt-7a modulates the synaptic vesicle cycle and synaptic transmission in hippocampal neurons. J Biol Chem 283(9):5918–5927. https://doi.org/10.1074/jbc.M705943200
14. Ciani L, Marzo A, Boyle K, Stamatakou E, Lopes DM, Anane D, McLeod F, Rosso SB et al (2015) Wnt signalling tunes neurotransmitter release by directly targeting Synaptotagmin-1. Nat Commun 6:8302. https://doi.org/10.1038/ncomms9302
15. Tabatadze N, Tomas C, McGonigal R, Lin B, Schook A, Routtenberg A (2012) Wnt transmembrane signaling and long-term spatial memory. Hippocampus 22(6):1228–1241. https://doi.org/10.1002/hipo.20991
16. Ochs SM, Dorostkar MM, Aramuni G, Schon C, Filser S, Poschl J, Kremer A, Van Leuven F et al (2015) Loss of neuronal GSK3beta reduces dendritic spine stability and attenuates excitatory synaptic transmission via beta-catenin. Mol Psychiatry 20(4):482–489. https://doi.org/10.1038/mp.2014.55
17. Tapia-Rojas C, Schuller A, Lindsay CB, Ureta RC, Mejias-Reyes C, Hancke J, Melo F, Inestrosa NC (2015) Andrographolide activates the canonical Wnt signalling pathway by a mechanism that implicates the non-ATP competitive inhibition of GSK-3beta: autoregulation of GSK-3beta in vivo. Biochem J 466(2):415–430. https://doi.org/10.1042/BJ20140207
18. Serrano FG, Tapia-Rojas C, Carvajal FJ, Hancke J, Cerpa W, Inestrosa NC (2014) Andrographolide reduces cognitive impairment in young and mature AbetaPPswe/PS-1 mice. Mol Neurodegener 9:61. https://doi.org/10.1186/1750-1326-9-61
19. Marzo A, Galli S, Lopes D, McLeod F, Podpolny M, Segovia-Roldan M, Ciani L, Purro S et al (2016) Reversal of synapse degeneration by restoring Wnt signaling in the adult hippocampus. Curr Biol 26(19):2551–2561. https://doi.org/10.1016/j.cub.2016.07.024
20. Fortress AM, Schram SL, Tuscher JJ, Frick KM (2013) Canonical Wnt signaling is necessary for object recognition memory consolidation. J Neurosci 33(31):12619–12626. https://doi.org/10.1523/JNEUROSCI.0659-13.2013
21. Ciani L, Boyle KA, Dickins E, Sahores M, Anane D, Lopes DM, Gibb AJ, Salinas PC (2011) Wnt7a signaling promotes dendritic spine growth and synaptic strength through Ca(2)(+)/Calmodulin-dependent protein kinase II. Proc Natl Acad Sci U S A 108(26):10732–10737. https://doi.org/10.1073/pnas.1018132108
22. Caceres A, Binder LI, Payne MR, Bender P, Rebhun L, Steward O (1984) Differential subcellular localization of tubulin and the microtubule-associated protein MAP2 in brain tissue as revealed by immunocytochemistry with monoclonal hybridoma antibodies. J Neurosci 4(2):394–410
23. Tapia-Rojas C, Burgos PV, Inestrosa NC (2016) Inhibition of Wnt signaling induces amyloidogenic processing of amyloid precursor protein and the production and aggregation of Amyloid-beta (Abeta)42 peptides. J Neurochem 139(6):1175–1191. https://doi.org/10.1111/jnc.13873
24. van de Wetering M, Cavallo R, Dooijes D, van Beest M, van Es J, Loureiro J, Ypma A, Hursh D et al (1997) Armadillo coactivates transcription driven by the product of the Drosophila segment polarity gene dTCF. Cell 88(6):789–799
25. Tapia-Rojas C, Lindsay CB, Montecinos-Oliva C, Arrazola MS, Retamales RM, Bunout D, Hirsch S, Inestrosa NC (2015) Is L-methionine a trigger factor for Alzheimer's-like neurodegeneration?: Changes in Abeta oligomers, tau phosphorylation, synaptic proteins, Wnt signaling and behavioral impairment in wild-type mice. Mol Neurodegener 10:62. https://doi.org/10.1186/s13024-015-0057-0

26. Koyama Y, Tohyama M (2012) A modified and highly sensitive Golgi-Cox method to enable complete and stable impregnation of embryonic neurons. J Neurosci Methods 209(1):58–61. https://doi.org/10.1016/j.jneumeth.2012.06.007
27. Niehrs C (2006) Function and biological roles of the Dickkopf family of Wnt modulators. Oncogene 25(57):7469–7481. https://doi.org/10.1038/sj.onc.1210054
28. Cross DA, Culbert AA, Chalmers KA, Facci L, Skaper SD, Reith AD (2001) Selective small-molecule inhibitors of glycogen synthase kinase-3 activity protect primary neurones from death. J Neurochem 77(1):94–102
29. Inestrosa NC, Varela-Nallar L (2015) Wnt signalling in neuronal differentiation and development. Cell Tissue Res 359(1):215–223. https://doi.org/10.1007/s00441-014-1996-4
30. Emami KH, Nguyen C, Ma H, Kim DH, Jeong KW, Eguchi M, Moon RT, Teo JL et al (2004) A small molecule inhibitor of beta-catenin/CREB-binding protein transcription [corrected]. Proc Natl Acad Sci U S A 101(34):12682–12687. https://doi.org/10.1073/pnas.0404875101
31. Yousif NG, Hadi NR, Hassan AM (2017) Indocyanine Green-001 (ICG-001) attenuates Wnt/beta-catenin-induces myocardial injury following sepsis. J Pharmacol Pharmacother 8(1):14–20. https://doi.org/10.4103/jpp.JPP_153_16
32. Risher WC, Ustunkaya T, Singh Alvarado J, Eroglu C (2014) Rapid Golgi analysis method for efficient and unbiased classification of dendritic spines. PLoS One 9(9):e107591. https://doi.org/10.1371/journal.pone.0107591
33. von Bohlen, Halbach O, Zacher C, Gass P, Unsicker K (2006) Age-related alterations in hippocampal spines and deficiencies in spatial memory in mice. J Neurosci Res 83(4):525–531. https://doi.org/10.1002/jnr.20759
34. Chen G, Chen KS, Knox J, Inglis J, Bernard A, Martin SJ, Justice A, McConlogue L et al (2000) A learning deficit related to age and beta-amyloid plaques in a mouse model of Alzheimer's disease. Nature 408(6815):975–979. https://doi.org/10.1038/35050103
35. Tapia-Rojas C, Inestrosa NC (2017) Wnt signaling loss accelerates the appearance of neuropathological hallmarks of Alzheimer's disease in J20-APP transgenic and wild-type mice. https://doi.org/10.1111/jnc.14278
36. Clevers H, Nusse R (2012) Wnt/beta-catenin signaling and disease. Cell 149(6):1192–1205. https://doi.org/10.1016/j.cell.2012.05.012
37. Jamieson C, Sharma M, Henderson BR (2012) Wnt signaling from membrane to nucleus: beta-catenin caught in a loop. Int J Biochem Cell Biol 44(6):847–850. https://doi.org/10.1016/j.biocel.2012.03.001
38. Cadigan KM, Waterman ML (2012) TCF/LEFs and Wnt signaling in the nucleus. Cold Spring Harb Perspect Biol 4 (11). https://doi.org/10.1101/cshperspect.a007906
39. Inestrosa NC, Varela-Nallar L (2014) Wnt signaling in the nervous system and in Alzheimer's disease. J Mol Cell Biol 6(1):64–74. https://doi.org/10.1093/jmcb/mjt051
40. Hall AC, Lucas FR, Salinas PC (2000) Axonal remodeling and synaptic differentiation in the cerebellum is regulated by WNT-7a signaling. Cell 100(5):525–535
41. Lucas FR, Salinas PC (1997) WNT-7a induces axonal remodeling and increases synapsin I levels in cerebellar neurons. Dev Biol 192(1):31–44. https://doi.org/10.1006/dbio.1997.8734
42. Farias GG, Valles AS, Colombres M, Godoy JA, Toledo EM, Lukas RJ, Barrantes FJ, Inestrosa NC (2007) Wnt-7a induces presynaptic colocalization of alpha 7-nicotinic acetylcholine receptors and adenomatous polyposis coli in hippocampal neurons. J Neurosci 27(20):5313–5325. https://doi.org/10.1523/JNEUROSCI.3934-06.2007
43. Wu D, Pan W (2009) GSK3: a multifaceted kinase in Wnt signaling. Trends Biochem Sci 35(3):161–168. https://doi.org/10.1016/j.tibs.2009.10.002
44. Oliva C, Vargas J, Inestrosa N (2013) Wnt signaling: role in LTP, neural networks and memory. Ageing Res Rev 12(3):786–800
45. Beique JC, Lin DT, Kang MG, Aizawa H, Takamiya K, Huganir RL (2006) Synapse-specific regulation of AMPA receptor function by PSD-95. Proc Natl Acad Sci USA 103(51):19535–19540. https://doi.org/10.1073/pnas.0608492103
46. Elias GM, Funke L, Stein V, Grant SG, Bredt DS, Nicoll RA (2006) Synapse-specific and developmentally regulated targeting of AMPA receptors by a family of MAGUK scaffolding proteins. Neuron 52(2):307–320. https://doi.org/10.1016/j.neuron.2006.09.012
47. Speese S, Budnik V (2007) Wnts: up-and-coming at the synapse. Trends Neurosci 30(6):268–275
48. Oliva CA, Inestrosa NC (2015) A novel function for Wnt signaling modulating neuronal firing activity and the temporal structure of spontaneous oscillation in the entorhinal-hippocampal circuit. Exp Neurol 269:43–55. https://doi.org/10.1016/j.expneurol.2015.03.027
49. Hooper C, Markevich V, Plattner F, Killick R, Schofield E, Engel T, Hernandez F, Anderton B et al (2007) Glycogen synthase kinase-3 inhibition is integral to long-term potentiation. Eur J Neurosci 25(1):81–86. https://doi.org/10.1111/j.1460-9568.2006.05245.x
50. Peineau S, Taghibiglou C, Bradley C, Wong TP, Liu L, Lu J, Lo E, Wu D et al (2007) LTP inhibits LTD in the hippocampus via regulation of GSK3beta. Neuron 53(5):703–717. https://doi.org/10.1016/j.neuron.2007.01.029
51. Mahmmoud RR, Sase S, Aher YD, Sase A, Groger M, Mokhtar M, Hoger H, Lubec G (2015) Spatial and working memory is linked to spine density and mushroom spines. PLoS One 10(10):e0139739. https://doi.org/10.1371/journal.pone.0139739
52. Leuner B, Falduto J, Shors TJ (2003) Associative memory formation increases the observation of dendritic spines in the hippocampus. J Neurosci 23(2):659–665
53. Jedlicka P, Vlachos A, Schwarzacher SW, Deller T (2008) A role for the spine apparatus in LTP and spatial learning. Behav Brain Res 192(1):12–19. https://doi.org/10.1016/j.bbr.2008.02.033
54. Beltran-Campos V, Prado-Alcala RA, Leon-Jacinto U, Aguilar-Vazquez A, Quirarte GL, Ramirez-Amaya V, Diaz-Cintra S (2011) Increase of mushroom spine density in CA1 apical dendrites produced by water maze training is prevented by ovariectomy. Brain Res 1369:119–130. https://doi.org/10.1016/j.brainres.2010.10.105
55. Moser MB, Trommald M, Andersen P (1994) An increase in dendritic spine density on hippocampal CA1 pyramidal cells following spatial learning in adult rats suggests the formation of new synapses. Proc Natl Acad Sci U S A 91(26):12673–12675
56. Fiala JC, Spacek J, Harris KM (2002) Dendritic spine pathology: cause or consequence of neurological disorders? Brain Res Brain Res Rev 39(1):29–54
57. Ehrlich I, Malinow R (2004) Postsynaptic density 95 controls AMPA receptor incorporation during long-term potentiation and experience-driven synaptic plasticity. J Neurosci 24(4):916–927. https://doi.org/10.1523/JNEUROSCI.4733-03.2004
58. Fitzgerald PJ, Pinard CR, Camp MC, Feyder M, Sah A, Bergstrom HC, Graybeal C, Liu Y et al (2015) Durable fear memories require PSD-95. Mol Psychiatry 20(7):901–912. https://doi.org/10.1038/mp.2014.161
59. Nagura H, Ishikawa Y, Kobayashi K, Takao K, Tanaka T, Nishikawa K, Tamura H, Shiosaka S et al (2012) Impaired synaptic clustering of postsynaptic density proteins and altered signal transmission in hippocampal neurons, and disrupted learning behavior in PDZ1 and PDZ2 ligand binding-deficient PSD-95 knockin mice. Mol Brain 5:43. https://doi.org/10.1186/1756-6606-5-43
60. Vargas JY, Fuenzalida M, Inestrosa NC (2014) In vivo activation of Wnt signaling pathway enhances cognitive function of adult mice and reverses cognitive deficits in an Alzheimer's disease model. J Neurosci 34(6):2191–2202. https://doi.org/10.1523/JNEUROSCI.0862-13.2014